Selective and Homo Emitter Junction Formation Using Precise Dopant Concentration Control by Ion Implantation and Microwave, Laser or Furnace Annealing Techniques

John Borland[1], Victor Moroz[2], Joanne Huang[2], John Chen[3], Yao-Jen Lee[4], Peter Oesterlin[5], Peter Venema[6], Henri Geerman[6], Peter Zhao[7] and Larry Wang[7]
[1]J.O.B. Technologies, Aiea, Hawaii, USA
[2]Synopsys, Mountain View, California, USA
[3]Kingstone, Shanghai, China
[4]National Nano Device Laboratories, Hsinchu, Taiwan
[5]Innovavent GmbH, Gottingen, Germany
[6]Tempress Systems B.V., Vaassen, the Netherlands
[7]Evans Analytical Group, Sunnyvale, California, USA

***Abstract*--- We investigated phosphorus and boon implanted emitter and selective emitter junction formation comparing; 1) 15keV to 30keV implant energies, 2) implant dopant dose concentration between 3E14/cm^2 to 1E16/cm^2 and 3) various anneal conditions from high temperature (>1407^{o}C) laser melt annealing to low temperature (<500^{o}C) microwave annealing and furnace anneals between 750^{o}C to 1050^{o}C for dopant activation and diffusion. By engineering and optimizing dopant concentration with anneals we could realize homo emitter and selective emitter junctions from 0.25um to 1.5um depth with sheet resistance from 9Ω/□ to 2200Ω/□ and peak surface dopant electrical activation levels from 4E18/cm^3 up to 5E20/cm^3. Highest dopant activation efficiency was achieved with liquid phase junction diffusion formation method using laser melt annealing and was limited by the dopant source concentration if <2E16/cm^2. The $POCl_3$ dopant source concentration of 1E16/cm^2 was only 15% efficient with furnace solid phase diffusion activation while laser melt liquid phase diffusion activation was 45% compared to implant which was 35% active with solid phase diffusion and 100% active with liquid phase diffusion.**

***Index Terms*--- dopant activation, ion implantation, laser anneal, liquid phase diffusion, microwave anneal, SIMS analysis, solid phase diffusion.**

I. INTRODUCTION

At the Sept. 2010 EU-PVSEC meeting, Jeon of Hyundai Heavy Industries [1] reported the comparison of $POCl_3$ to phosphorus (P) implant emitter doping with laser edge isolation showing no difference in cell efficiency going from 17.85% to 17.86%, however when they eliminated the laser edge isolation with P-implant cell efficiency improved by 0.35% to 18.21%. They also investigated a highly doped P-implanted selective emitter of 60Ω/□ compared to a homo emitter P-implanted emitter region of 100Ω/□ and they only observed a +0.14% cell efficiency improvement going from 18.36% to 18.50%. Similarly in Nov. 2010 Rohatgi of Suniva [2] reported on the 1st production replacement of $POCl_3$ diffusion doped emitters with P-implanted and diffused emitters improving the total cell efficiency by 1% from 18.0% to 19.0%. However, with a P-implanted and diffused selective emitter they also reported only a very small 0.1% cell efficiency improvement to 19.1%. Other selective emitter doping methods such as localized dopant paste by Innovalight [3, 4] or localized-laser-melt (LLM) annealing by Suntech-Power [5] have reported much higher cell efficiency improvements from 1% to 2%. These differences could be due to differences in dopant activation level limited by dopant solid solubility in silicon based on the annealing temperature and or differences in the dopant concentration available from the particular dopant source as reported by Palina [6] who compared B-SOD (boron-spin-on-dopant) 0.4mg to 28.2mg resulting in Rs (sheet resistance) from 50 Ω/□ to 8 Ω/□ respectively with LLM annealing. Hameiri of Univ. of New South Wales [7] also reported inconsistent B-SOD concentration results, 4% B-SOD Rs was 10 Ω/□, 8% was 80 Ω/□ and 10% was 38 Ω/□ suggesting poor B concentration control and precision with their Filmtronics B-SOD. Therefore, using the precision of accurate dose control by implantation in this study we investigated precise dopant concentration effects for both phosphorus and boron implantation over the dose range from 3E14/cm^2 to 1E16/cm^2 with various annealing conditions for emitter junction formation to realize high dopant activation efficiency including lower temperatures down

to 600°C anneals as reported earlier by Tokiguchi of Hitachi [8].

II. EXPERIMENTATION

Four different P and B implant doses (concentrations) were examined 3E14/cm^2, 1E15/cm^2, 3E15/cm^2 and 1E16/cm^2 at two different implant energies 15keV and 30keV provided by Kingstone in Shanghai, China. Based on solid phase diffusion, junction annealing simulations provided by Synopsys we selected furnace annealing at 750°C for 60 minutes, 850°C for 30 minutes and 1050°C for 10 minutes provided by Tempress in the Netherlands using their horizontal diffusion furnaces with a thin 3-5nm surface oxide cap grown at a low temperature. Since high dose implants can be self-amorphizing we also looked at low temperature microwave annealing at 500°C for 5 minutes at two different power settings for SPE (solid phase epitaxy) dopant activation using the DSG microwave annealer at National Nano Device Lab in Hsinchu, Taiwan. For localized selective emitter formation we used LLM annealing provided by Innovavent GmbH in Gottingen, Germany using a 300ns pulse green laser anneal at 1, 3, 5 and 6.7 J/cm^2 power levels for LPE (liquid phase epitaxy) or liquid phase dopant diffusion. Evans Analytical Group provided SIMS analysis of the LLM regions for dopant depth profiles and detection of other impurities such as segregation of the surface oxide into the melt region and areal density measurements. ECV carrier depth profiles were measured by Tempress. Fig.1 shows the overall implant and annealing experimental matrix. Tempress also provided the $POCl_3$ and BBr_3 doped wafers.

Species	Dose	Energy	Microwave	750C	850C	1050C	Laser=	1J	3J	5J	6.7J
B	3E14	15keV	X	X	X	X		X	X	X	X
B	3E14	30keV	X	X	X	X		X	X	X	X
B	1E15	15keV	X	X	X	X		X	X	X	X
B	1E15	30keV	X	X	X	X		X	X	X	X
B	3E15	15keV	X	X	X	X		X	X	X	X
B	3E15	30keV	X	X	X	X		X	X	X	X
B	1E16	15keV	X	X	X	X		X	X	X	X
B	1E16	30keV	X	X	X	X		X	X	X	X
P	3E14	15keV	X	X	X	X		X	X	X	X
P	3E14	30keV	X	X	X	X		X	X	X	X
P	1E15	15keV	X	X	X	X		X	X	X	X
P	1E15	30keV	X	X	X	X		X	X	X	X
P	3E15	15keV	X	X	X	X		X	X	X	X
P	3E15	30keV	X	X	X	X		X	X	X	X
P	1E16	15keV	X	X	X	X		X	X	X	X
P	1E16	30keV	X	X	X	X		X	X	X	X
POCl3	→							X	X	X	X
BBr3	→							X	X	X	X

Fig.1: Implant and anneal matrix.

III. RESULTS

A. Junction Simulation

The as implanted junction depth for P at 15keV is ~0.2um and at 30keV is ~0.3um while for B at 15keV is ~0.25um and at 30keV is ~0.38um as shown in Fig2 a-d and the effects of annealing temperature (800°C, 900°C and 1000°C) and annealing time (0.1sec to 30mins) are also shown in the junction depth simulation results. Solar cell efficiency simulation results from Synopsys in Fig.3 shows that high surface dopant levels leads to low resistance but also low surface lifetime so shallow junction <0.1um is better while low surface dopant levels leads to higher surface resistance but also higher surface lifetime so deeper junctions >0.8um are preferred [9]. Typical industry standard $POCl_3$ junctions of 0.3-0.6um deep and 1-3E20/cm^3 surface dopant levels are high-lighted in yellow in Fig.3 while improved junctions are high-lighted in red. For implanted and shallow solid phase diffused junctions the annealing temperature determines the surface dopant activation level due to dopant solid solubility limit in silicon with the excess chemical dopant electrically inactive degrading surface lifetime. For deeper junctions the available dopant concentration/dose limits the surface activation level resulting in 100% dopant activation. This is clearly seen in Fig.4 comparing B=1E16/cm^2 900°C solid phase diffused junction simulation results at 10sec, 5min. and 30min anneal times showing the boron dopant solid solubility limit (Bss) is ~7E19/cm^3 and the peak B chemical level is >2E21/cm^3 so all the excess B dopant is electrically inactive. Fig. 5 is for the 1000°C anneal temperature which increase Bss to 1.5E20/cm^3 and the higher temperature with deeper B diffusion depletes the surface of most of the excess chemical B to <5E20/cm^3. The maximum B dopant solid solubility limit in silicon at melting temperature (1407°C) is 6E20/cm^3. Phosphorus dopant solid solubility limit (Pss) in silicon is much higher than B, at 800°C Pss is ~2.5E20/cm^3, at 900°C Pss is ~5E20/cm^3, at 1000°C Pss is ~6E20/cm^3 and at 1407°C (melt temperature) Pss is ~1.5E21/cm^3 so laser melt annealing with liquid phase dopant diffusion is required to achieve highest efficiency P or B emitter dopant activation.

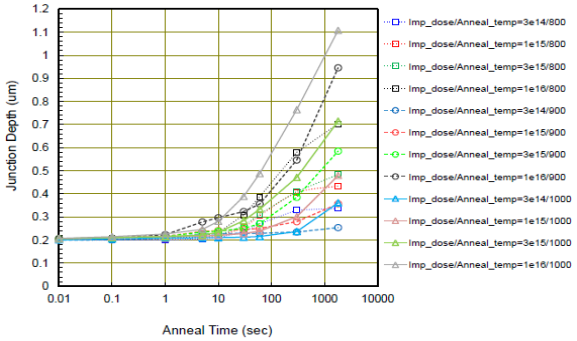

Fig.2a: P 15keV junction simulation results.

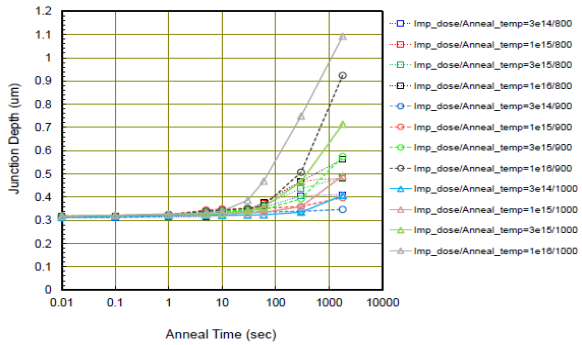

Fig.2b: P 30keV junction simulation results.

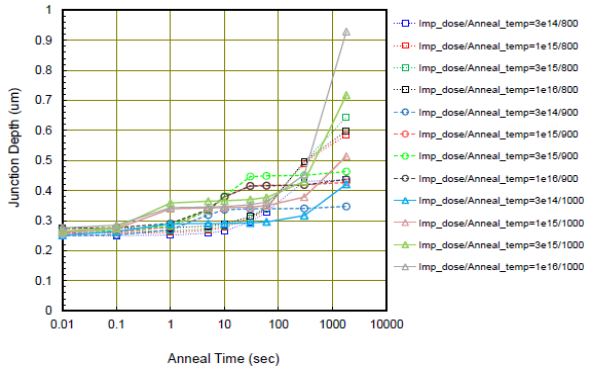

Fig.2c: B 15keV junction simulation results.

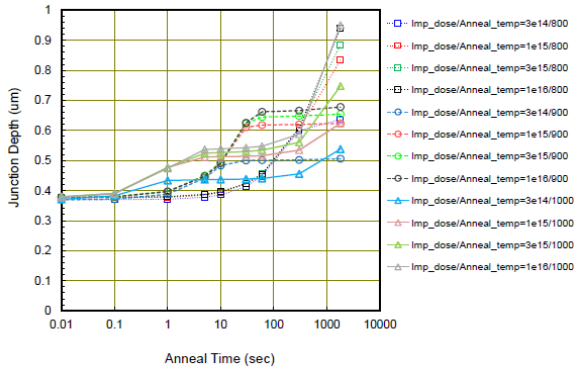

Fig.2d: B 30keV junction simulation results.

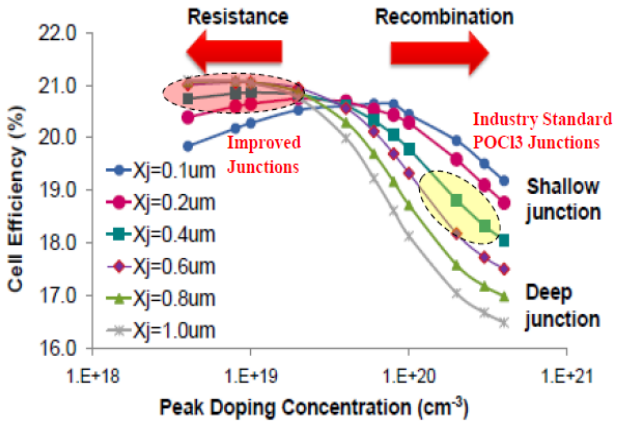

Fig.3: Simulation results showing cell efficiency versus emitter peak doping level and junction depth.

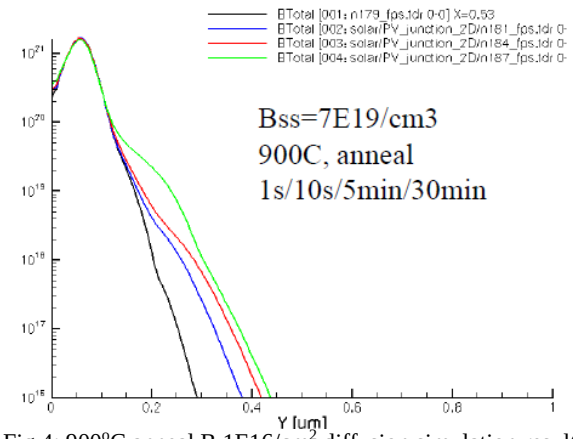

Fig.4: 900°C anneal B 1E16/cm^2 diffusion simulation results.

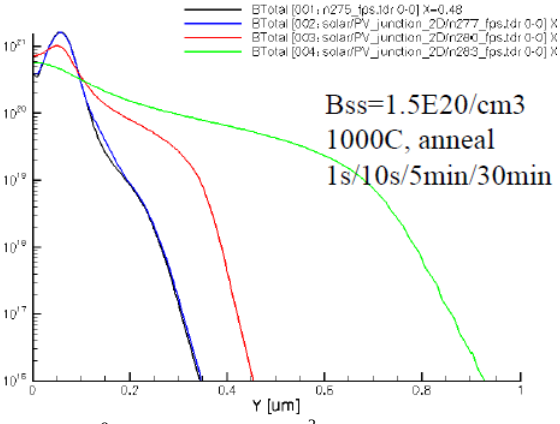

Fig.5: 1000°C anneal B 1E16/cm^2 diffusion simulation results.

B. Phosphorus Implantation

The Rs results for the 15keV and 30keV P-implants are shown in Fig.6 for the various annealing conditions. Surprising is that the 5min. microwave anneal Rs results are better than the 750°C 90min and 850°C 60min furnace

anneals at the lower 3E14/cm^2 and 1E15/cm^2 doses. The P-implant is self-amorphizing so SPE dopant activation dominates and the Rs results are dose limited at these low temperatures and doses. But P-dopant activation becomes temperature limited due to Pss at doses >2E15/cm^2. For the high temperature anneals at 1050^{o}C and 1407^{o}C the P-implant activation level was still dose limited beyond 1E16/cm^2 and the 15keV P-implants show slightly higher Rs than 30keV P-implants. Fig.7 shows the 15keV 1E16/cm^2 dose P dopant profiles comparing liquid phase diffusion for LLM annealing using P-SIMS depth profile while solid phase diffusion for furnace annealing using P-ECV profile. The LLM process results in 100% P-implant dopant activation and low Rs of 16Ω/□ at 3J/cm^2 with P SIMS areal density of 9.2E15/cm^2 and 12Ω/□ at 5J/cm^2 with P SIMS areal density of 1.04E16/cm^2. The flat peak P SIMS dopant level is 5E20/cm^3 for 3J and 3E20/cm^3 for 5J both well below the melt Pss limit of 1.5E21/cm^3. The ECV P flat peak electrical dopant level for both the 750^{o}C and 850^{o}C furnace anneals were 5.5E20/cm^3 well above the theoretical Pss level of 2-3E20/cm^3 but the Rs values were high at 90Ω/□ for an P dopant electrical activation concentration of 9E14/cm^2 (9%) at 750^{o}C and 30Ω/□ for 3E15/cm^2 activated dopant concentration (30%) at 850^{o}C. At 1050^{o}C the 10Ω/□ corresponds to 1E16/cm^2 activated dopant concentration (100%) like with LLM and a surface Pss~3E20/cm^3 due to the deep junction diffusion of 1.5um. The P and O SIMS depth profiles for the 3E14/cm^2, 3E15/cm^2 and 1E16/cm^2 doses for the 3 & 5J/cm^2 LLM anneals are shown in Fig.8. The 3E14/cm^2 dose melt process results in a P flat doping level of 1.8E19/cm^3 with Rs=226Ω/□, the 3E15/cm^2 dose P flat doping level is 2.0E20/cm^3 with Rs=34Ω/□ and the 1E16/cm^2 dose P flat doping level is 5E20/cm^3 with Rs=16Ω/□ with junction depth ~0.3-0.35um for the 3J/cm^2 and 0.7-0.85um for 5J/cm^2 LLM. Note that the oxygen (O) SIMS analysis shows that the surface oxide mixes with the silicon melted region to the 0.25um melt depth at 3J/cm^2 and 0.55um melt depth at 5J/cm^2 with a low O areal density of 2.8-3.8E14/cm^2 at a level of 3-4E18/cm^3. At the melting temperature of silicon (1407^{o}C) Pss=1.5E21/cm^3 and that would suggest we can triple the P-implant dose concentration to 3-4E16/cm^2 to achieve the maximum Pss melt level of 1.5E21/cm^3 and Rs of 2-3Ω/□.

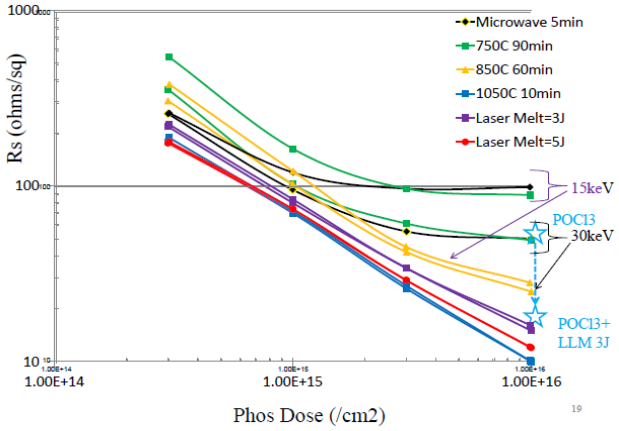

Fig.6: Rs versus P implant dose and annealing condition.

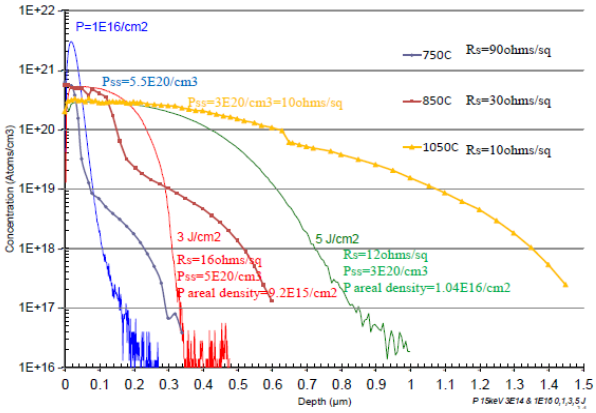

Fig.7: P 1E16/cm2 SIMS liquid phase diffusion and ECV solid phase diffusion profiles.

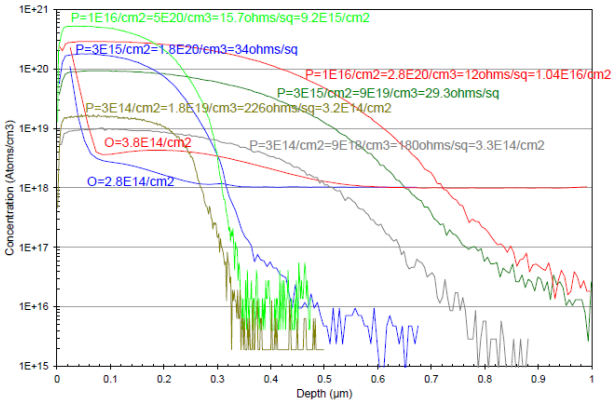

Fig.8: P and oxygen SIMS profile for laser melt liquid phase diffusion.

Most $POCl_3$ doping is typically 60-70Ω/□ at 850^{o}C and with LLM this is reduced to 20-30Ω/□ [10] suggesting a total equivalent P doping dose concentration of ~5E15/cm^2 based on Fig.6 so for comparison we also evaluated a standard $POCl_3$ wafer from Tempress. The P SIMS areal density measurements of $POCl_3$ shows total P

concentration SIMS areal density of 1.08E16/cm^2 in Fig.9 but only 4.4E15/cm^2 P was diffused into the silicon with 5.6E15/cm^2 P still remaining in the surface $POCl_3$ oxide layer after diffusion. The $POCl_3$ diffusion Rs value of 68Ω/□ suggests that only 1.5E15/cm^2 P concentration is electrically active, ~15% as shown in Fig.6. We also measured the surface oxide O-SIMS areal density for $POCl_3$ which is 7E16/cm^2 as shown in Fig.9 or about 222 monolayer thick (70nm) and after 3J/cm^2 LLM Rs improves to 23Ω/□ or 5.5E15/cm^2 P dopant activation concentration level in Fig.6 with SIMS P areal density of 6.5E15/cm^2 in silicon and 1.7E15/cm^2 remaining in the surface oxide with O areal density of 8E16/cm^2. The Pss level is 3.5E20/cm^3 with a slight increase in junction depth to 0.42um. The high O SIMS areal density detected and profiles in Fig.9 shows evidence that the surface oxide segregates and is incorporated into the melt region to the melt depth of 0.25um or 0.5um at an O level of 3-4E18/cm^3 suggesting that nitrogen from a surface SiN/ARC layer may behave similarly as reported by Xu of PARC [11] and may be an issue for LLM after SiN/ARC. Also, based on the 850^{o}C Rs results in Fig.6 the P-implant Rs results reported by Jeon [1] of 100Ω/□ would correspond to a 1E15/cm^2 dose concentration while 60Ω/□ would be 2E15/cm^2 dose concentration.

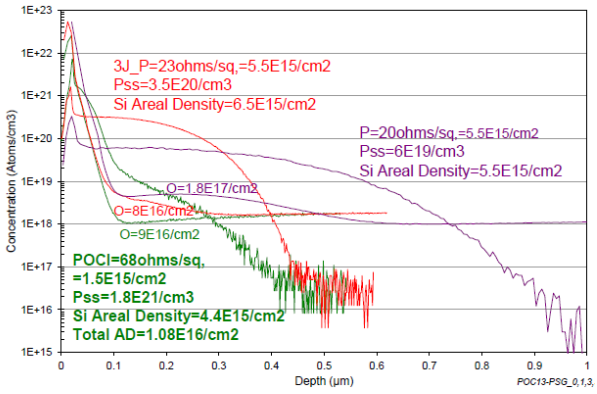

Fig.9: POCl3 P and O SIMS profiles for liquid phase diffusion.

C. Boron Implantation

The Rs results versus B-implant dose for the 15keV and 30keV conditions are shown in Fig.10. This time the microwave anneals gave the highest Rs values followed by the 750^{o}C and then the 850^{o}C furnace anneals while the high temperature 1050^{o}C and laser melt anneal Rs values were similar and implant dose limited (limited to available dopant concentration) and not anneal temperature. The deeper 30keV B-implant Rs values were slightly lower than the 15keV implant results. The 3 & 5J/cm^2 laser melt B-SIMS results are shown in Fig.11 and the peak B-flat doping level in the melt liquid phase diffusion region is 1.5E19/cm^3 for the low 3E14/cm^2 dose at 3J-LLM with Rs=324Ω/□ and Xj~0.4um while at 5J-LLM Xj increases to 0.7um with Rs=279Ω/□ and peak B-flat level of 8E18/cm^3. For the high 1E16/cm^2 dose at 3J-LLM peak B-flat level is 3E20/cm^3 with Rs=16Ω/□ and a 0.4um junction depth. These B concentration levels are far below the 6E20/cm^3 Bss limit at the melt temperature of silicon suggesting a higher B-dose of 2.2E16/cm^2 should be investigated to maximize the benefits of using laser melt selective emitter processing for highest dopant activation efficiency with a 0.4um junction at 6 Ω/□ as shown in Fig.12 based on the melt temperature Bss limit of 6E20/cm^3. Based on Fig.10 and the B Rs results reported earlier by Palina [6] the 28.2mg B-SOD sample of 8 Ω/□ should have a B activated dopant concentration equivalent to 1.8E16/cm^2 dose and the 0.4mg 50 Ω/□ sample equivalent would be 3.0E15/cm^2 activated dose. Applying the Fig10 Rs concentration results to Hameiri [7] B-SOD Rs results would suggest the 8% B-SOD with Rs=80Ω/□ has a B electrically activated concentration equivalent to 1.5E15/cm^2 dose, 10% B-SOD with Rs=38Ω/□ has B activation concentration of 3.0E15/cm^2 and the 4% B-SOD with Rs=10Ω/□ has the highest B activation concentration of 1.7E16/cm^2. Therefore, 8% B-SOD=B*, 10% B-SOD=2xB* and 4% B-SOD=11xB*.

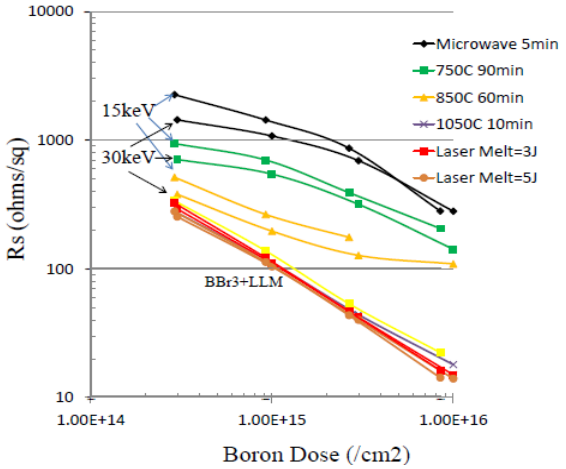

Fig.10: Rs versus B implant dose and anneal condition.

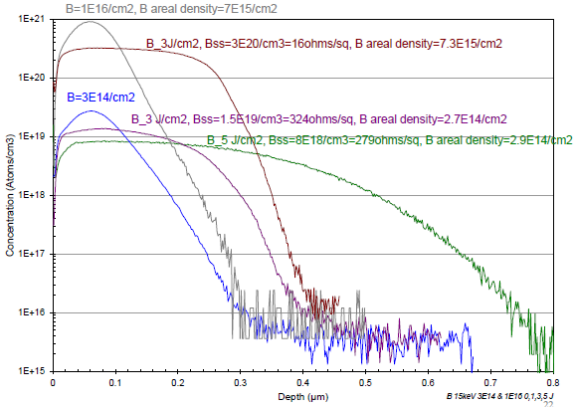

Fig.11: B and oxygen SIMS profile for laser melt anneal.

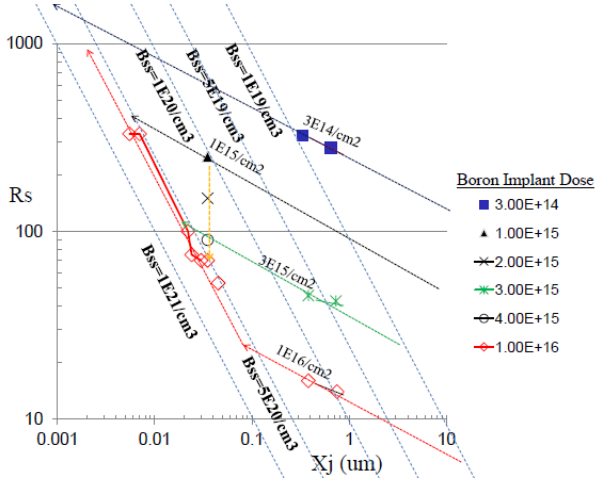

Fig.12: Rs versus B junction depth and dose with Bss limits.

D. P and B Implant Dose Comparison

A direct comparison of Rs between P and B implant dose at 30keV for the various annealing conditions is shown in Fig.13 below. The limitation of dopant activation due to solid solubility with annealing temperature especially for B dopant can clearly be seen when using furnace anneal solid phase diffusion compared to laser melt liquid phase diffusion.

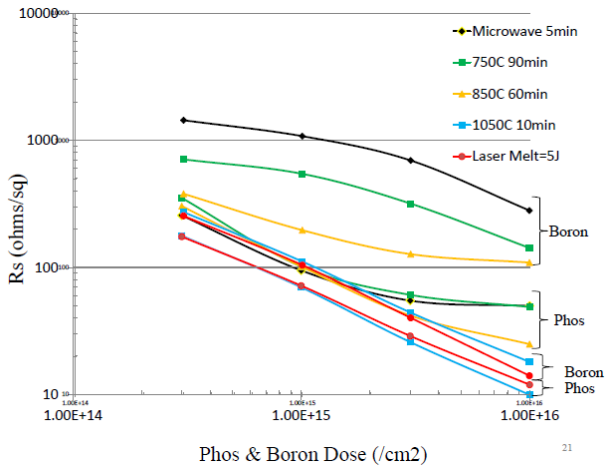

Fig.13: Rs versus P and B dose at 30keV for various anneals.

IV.SUMMARY

We achieved precise surface dopant concentration and activation control using ion implantation with various annealing techniques from 4E18/cm^3 (2200Ω/□) with an implant dose of 3E14/cm^2 to 5E20/cm^3 (10Ω/□) with a dose of 1E16/cm^2. $POCl_3$ dopant activation by solid phase diffusion was only 15% efficient/active while liquid phase diffusion was 45% efficient/active. To see the full benefit of localized laser melt annealing for selective emitter to maximize dopant activation based on solid solubility limit higher selective emitter P and B dopant sources should be investigated in the future with an equivalent dose concentration of 2-3E16/cm^2 range for highest dopant activation efficiency with Rs 3-6Ω/□ by laser melt liquid phase dopant diffusion. This will realize a Pss limit of ~1.5E21/cm^3 and a Bss limit of ~6E20/cm^3.

ACKNOWLEDGEMENT

We are grateful to James Hwang and J. S. Whang of Amtech Systems for their support of this study.

REFERENCES

[1] M. Jeon et al., "Emitter Formation Using Ion Implantation Method for Fabrication of Crystalline Silicon Solar Cells", 2010 EU-PVSEC, paper 2DV.1.3.

[2] A. Rohatgi and D. Meier, "Developing Novel Low-Cost, High-Throughput Processing Techniques for 20% Efficient Monocrystalline Silicon Solar Cells", Photovolatics International, Nov. 2010, p.87.

[3] D. Poplavskyy et al., "Silicon Ink Selective Emitter Process: Optimization of Selectively Diffused Regions for Short Wavelength Response", IEEE-PVSC 2010, paper 928.

[4] K. Alberi et al., "Localized Doping Using Silicon Ink Technology for High Efficiency Solar Cells", IEEE-PVSC 2010, paper 334.

[5] Z. Shi et al., "Mass Production of the Innovative Pluto Solar Cell Technology", www.Suntech-power.com web-site white paper.

[6] N. Palina et al., "Laser Assisted Boron Doping of Silicon Wafer Solar Cells Using Nanosecond and Picosecond Laser Pulses", IEEE-PVSC 2011, paper 633.

[7] Z. Hameiri et al., "Laser Doped Local Back Surface Field", IEEE-PVSC 2011, paper 321.

[8] K. Tokiguchi et al., "Silicon Solar Cell Fabricated by Ion Implantation", Semiconductor Technologies (1984), p.235.

[9] V. Moroz, "Modeling and Optimization of Silicon Solar Cells", presentation material from the NCCAVS User Group Conference on PV Technology, Feb. 23, 2011.

[10] U. Jaeger et al., "Beam Shaping-The Key To High Throughput Selective Emitter Laser Processing With A Single Laser System", IEEE-PVSC 2010, paper 320.

[11] B. Xu et al., "Front Side Metallization of Crystalline Silicon Solar Cells Using Selectively Laser Drilled Contact Openings", IEEE-PVSC 2009, p.517.